Clinical Oral Investigations
https://doi.org/10.1007/s00784-021-03956-y

ORIGINAL ARTICLE

Computed tomography and histological evaluation of xenogenic and biomimetic bone grafts in three-wall alveolar defects in minipigs

Yago Raymond[1,2] · David Pastorino[1] · Ignacio Ginebreda[3] · Yassine Maazouz[1] · Mònica Ortiz[2] · Maria-Cristina Manzanares[4] · Maria-Pau Ginebra[1,2,5]

Received: 13 November 2020 / Accepted: 19 April 2021

Abstract

Objectives This study aimed to compare the performance of a xenograft (XG) and a biomimetic synthetic graft (SG) in three-wall alveolar defects in minipigs by means of 3D computerised tomography and histology.

Materials and methods Eight minipigs were used. A total of eight defects were created in the jaw of each animal, three of which were grafted with XGs, three with SGs, and two were left empty as a negative control. The allocation of the different grafts was randomised. Four animals were euthanised at 6 weeks and four at 12 weeks. The grafted volume was then measured by spiral computed tomography to assess volume preservation. Additionally, a histological analysis was performed in undecalcified samples by backscattered scanning electron microscopy and optical microscopy after Masson's trichrome staining.

Results A linear mixed-effects model was applied considering four fixed factors (bone graft type, regeneration time, anatomic position, and maxilla/mandible) and one random factor (animal). The SG exhibited significantly larger grafted volume (19%) than the XG. The anterior sites preserved better the grafted volume than the posterior ones. Finally, regeneration time had a positive effect on the grafted volume. Histological observations revealed excellent osseointegration and osteoconductive properties for both biomaterials. Some concavities found in the spheroidal morphologies of SGs were associated with osteoclastic resorption.

Conclusions Both biomaterials met the requirements for bone grafting, i.e. biocompatibility, osseointegration, and osteoconduction. Granule morphology was identified as an important factor to ensure a good volume preservation.

Clinical relevance Whereas both biomaterials showed excellent osteoconduction, SGs resulted in better volume preservation.

Keywords Bone regeneration · In vivo · Miniature swine · Bone graft · Xenograft · Synthetic graft

✉ Maria-Pau Ginebra
maria.pau.ginebra@upc.edu

[1] Mimetis Biomaterials S.L., Carrer de Cartagena, 245, 3F, 08025 Barcelona, Spain

[2] Biomaterials, Biomechanics and Tissue Engineering Group, Department of Materials Science and Engineering, Universitat Politècnica de Catalunya (UPC), EEBE, Av. Eduard Maristany, 10-14, 08019 Barcelona, Spain

[3] Department of Restorative and Esthetic Dentistry, Universitat Internacional de Catalunya, Carrer de Josep Trueta, 08195 Sant Cugat del Vallès, Barcelona, Spain

[4] Human Anatomy and Embryology Unit, Department of Pathology and Experimental Therapeutics, Universitat de Barcelona, 08907 L'Hospitalet de Llobregat, Barcelona, Spain

[5] Institute for Bioengineering of Catalonia (IBEC), Barcelona Institute of Science and Technology, C/ Baldiri Reixac 10-12, 08028 Barcelona, Spain

Introduction

Bone loss continues to be a major clinical burden in the dental field, especially in cases where tooth extraction is not quickly followed by the placement of an implant. In this case, the lack of local mechanical stimulation leads to considerable bone resorption [1]. During this process, the bundle bone, i.e. the bone that surrounds the tooth and contains the periodontal ligament fibres binding the tooth to the bone, is no longer necessary and is progressively resorbed and replaced by woven bone [2]. This results in an accentuated vertical reduction of the buccal alveolar crest, which is exclusively composed of bundle bone. Simultaneously, there is a resorption of the outer surfaces of both the buccal and the lingual bone walls, which greatly reduces the amount of bone to successfully place an implant with lasting benefits [2]. In these situations, bone augmentation is a widely used solution [3].

Published online: 01 May 2021

Bone grafts (BGs) are used to fill bone defects and support bone regeneration in the grafted volume. The aim is often to achieve the volume required to place a stable dental implant. BGs are available in different shapes and delivery systems such as granules, blocks, or putties [4]. In the dental field, granules are the most common option for the treatment of walled bone defects [5]. BGs can be classified, based on their origin, as autografts, allografts, xenografts, or synthetic grafts [6, 7]. Since their introduction in the 1970s, synthetic BGs have progressively evolved, and different strategies have been tried to improve their biological performance. One of the strategies that has recently been proposed is based on the development of biomimetic materials, which are synthesised using mild processing conditions instead of the traditional high-temperature ceramic methods. This results in a material that is considerably more similar to the mineral phase of bone, not only in terms of composition but also in terms of microstructure and reactivity [8]. In previous studies, it has been shown that biomimetic calcium phosphates have very interesting properties in terms of osteoimmunomodulation [9], in vivo osteoconductivity [10], and osteoinductivity [11]. However, there still exists a lack of information regarding the efficacy of these biomimetic materials compared to the xenogenic grafts in clinically relevant defects for dental applications in large animals.

The clinical success of a bone grafting procedure is linked to the preservation of the grafted volume. This is achieved by preventing a short-term volume loss [12, 13] and promoting the long-term remodelling of the graft into the vascularised bone, without compromising the volume [14]. The regeneration process associated with a bone graft depends on numerous factors. Recent studies have demonstrated that it largely depends on the carefully coordinated interactions between various cell types, including immune, endothelial, and bone cells [15]. Whilst a certain degree of inflammation has been shown to trigger the bone regeneration cascade, the benefits of early inflammation are to be contained, as excessive or prolonged inflammation may result in a suboptimal bone formation [16]. Moreover, a high vascularisation is required to guarantee the oxygen and nutrient supply to the highly metabolically active cells involved in tissue regeneration [17]. The features of bone grafts are known to play a crucial role in the modulation of all these biological processes [8]. Not only composition matters but also textural properties are important. Achieving the adequate porosity is necessary to promote vascularisation and tissue colonisation, enhancing the interaction of the material with the host tissue [18, 19]. Finally, the graft must have the appropriate mechanical properties to guarantee the preservation of the biomechanical functions of bone during the healing process, thus avoiding both weakening and stress shielding effects [20].

The present work focuses on the comparative evaluation of two bone substitutes with different origins: a synthetic biomimetic calcium phosphate (MimetikOss®, Mimetis Biomaterials, Spain) and a deproteinised bovine bone matrix (Bio-Oss®, Geistlich Biomaterials, Switzerland). For this purpose, the volume preservation and tissue regeneration processes were evaluated after 6 and 12 weeks of healing in three-wall bone defects created in the mandible and maxilla of minipigs grafted with the two different materials.

Materials and methods

Bone grafts

Two types of bone grafts were used to fill the defects:

- A control group being a xenograft (XG) from bovine origin (Bio-Oss®, Geistlich Biomaterials, Switzerland) in granular form with sizes between 0.25 and 1 mm and;
- A test group being a synthetic biomimetic graft (SG) processed at low temperature and composed of 80% biomimetic calcium deficient hydroxyapatite and 20% β-tricalcium phosphate (MimetikOss®, Mimetis Biomaterials, Spain) in granular form with sizes between 0.2 and 1 mm.

Both biomaterials were commercially available in vials sealed into blisters, provided in sterile conditions, and used appropriately by following their instructions for use. The physicochemical properties of the two grafting materials are described in a previous study [21].

Animals

Eight landrace minipigs (6-month-old, mixed sexes and from 18 to 31 kg) were provided by a GLP clinical research organisation (CRO) (Specipig S.L., Barcelona, Spain). The animals were kept in presurgical housing for 1 week.

Study design

The study was conducted complying with the EU Directives 2004/10/EU, 2010/63/EU and the Spanish law RD 1369/2000 regarding the protection of animals used for scientific purposes. The experiments were carried out at the GLP facilities of the CRO and were reviewed and approved by the Specipig Ethics Committee for Animal Experimentation. The surgical procedure was performed by I.G.

The indication chosen was the regeneration of a three-wall defect in the alveolar ridge, which is one of the most common surgical procedures in modern dentistry [22].

Eight defects were created per animal in the surgical sites indicated in Fig. 1a and referenced accordingly. For each animal, three defects were filled with XGs, three with SGs, and two were left empty. The distribution of the grafts and the

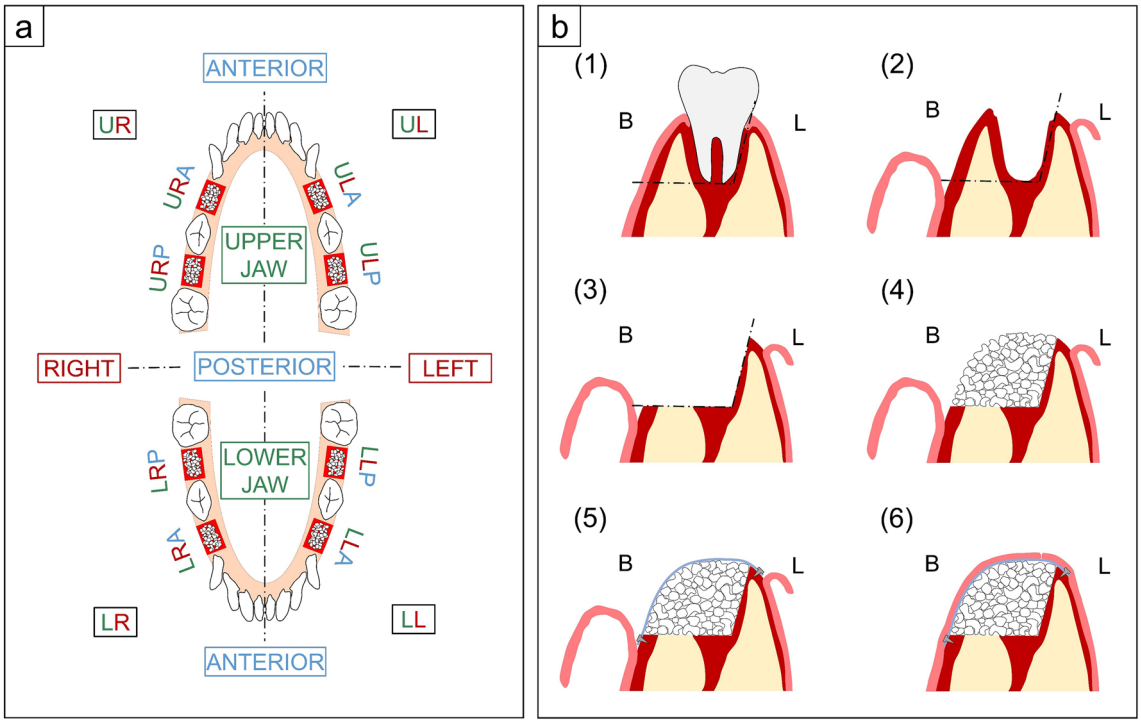

Fig. 1 **a** Scheme of the created defects and reference names. Coronal plane projection of the upper (U) and lower (L) jaw. L and R stand for left and right and M and D stand for mesial and distal anatomic sites, respectively. **b** Procedure to create the standardised three-wall bone defect, grafting, and suturing: (1) Initial situation, (2) tooth extraction and rising of the flap, (3) creation of the three-wall bone defect by removing the buccal alveolar ridge, (4) grafting of the defect, (5) covering the graft with a collagen membrane, and (6) stitching the gingiva. B and L stand for buccal and lingual sides, respectively

empty defects was defined in a balanced manner (i.e. altogether, each biomaterial was grafted the same number of times in each of the eight surgical sites) and randomly assigned to the animals. All defects were then covered with resorbable collagen membranes (Creos Xenoprotect, Nobel Biocare, Switzerland). Two time points were evaluated: 6 and 12 weeks. At each time point, four animals were euthanised, which gave 12 replicates per material and time point.

Computerised tomography (CT) of each animal was performed postoperatively and at the time of euthanasia. Additionally, the grafted regions were explanted and processed for histological evaluation.

Surgical procedure

Anaesthesia and medication

A premedication of 0.04 mg/kg of atropine was administered intramuscularly (IM) in the neck. Using the same method, sedation was achieved with 0.020 to 0.035 mg/kg of dexmedetomidine and 0.08 to 0.30 mg/kg of midazolam combined with 0.15 to 0.30 mg/kg of butorphanol as an analgesic. After 15–20 min, an intravenous (IV) catheter was placed in order to continue with IV fluid therapy using ringer lactate serum combined with the medication. Animals were then preoxygenated with 100% oxygen for 3 min. Propofol of 1.5 to 5.0 mg/kg was administered through IV injection. Endotracheal intubation was performed using isoflurane with a minimum alveolar concentration of 1.2–2.4% and 2% oxygen. Immediately after surgery, a nonsteroidal anti-inflammatory (meloxicam 0.4 mg/kg IM in the neck muscles) and a general antibiotic coverage (enrofloxacin from 2.5–5 mg/kg IM in the neck muscles) were administered.

Tooth extraction and creation of the defect

Right before starting the surgical procedure, the oral cavity was scrubbed with 10% iodine povidone. Additionally, the teeth to be removed were manually scaled, and calculus was eliminated. Then, a full-thickness flap from the first premolar to the most distal molar was raised both buccally and lingually as seen in Fig. 1b-2. Eight three-wall bone defects were shaped after tooth extraction by removing the buccal plate to half of its height as illustrated in Fig. 1b-3. The removed teeth were the first and third premolars of the lower quadrants and the first premolar and first molar of the upper quadrants. A periodontal probe and a high-speed handpiece under copious irrigation were utilised to create the standard-sized alveolar defects. The size of the defects was 12 mm in depth and 10 mm in width.

Grafting

BGs were first hydrated with Ringer's solution and then placed in the defects by gently packing to achieve the best volume filling (Fig. 1b-4). Then, a collagen resorbable membrane was cut and adapted to the size of the defect. The wound was prepared for tension-free closure by releasing the periosteum underneath the flap. Primary closure was achieved in all cases with 4-0 Vicryl® degradable braided suture (polyglactin 910, Johnson & Johnson, USA). Horizontal mattress and single interrupted sutures were used to close the wound (Fig. 1b-5 and b-6).

Post-operative

After the surgery, butorphanol was administered IM 0.15–0.30 mg/kg every 12 h as an analgesic for 2 days. Anti-inflammatory treatment with meloxicam was administered IM 0.4 mg/kg every 24 h for 5 days. Antibiotic treatment with enrofloxacin was administered IM 2.5–5.0 mg/kg every 24 h for 5 days post-surgery. One week after the surgical procedure, animals were sedated and wounds were reviewed to look for any possible events that would compromise healing and overall results. No screaming nor altered behaviour was registered. No bleeding nor vocalisation was observed or heard during the 2 weeks following the surgeries.

Monitoring

The minipigs were maintained on a soft diet for 48 h after the surgery. Animal weight was tracked weekly. All the animals showed a proper evolution. In addition, the specimens were observed twice a day for any abnormality.

Computerised tomography

An initial CT scan was registered for each animal one day after the surgery (Philips IQUON CT-SCAN, Royal Philips, the Netherlands). A second CT scan was performed before euthanasia at 6 or 12 weeks depending on the group. Stacks of images were acquired with an isotropic pixel size of 500 μm. Slices were performed in the coronal plane and through the whole range of the mandible and maxilla (Fig. 2).

Volumetric CT quantification

A sample of each BG was scanned and used to determine the radiopacity thresholds of each biomaterial. Ranges of 442–948 HU and 847–1435 HU were established for XG and SG, respectively. Then, the defect regions were identified by a trained observer based on the recognition of its anatomical location. The grafted volume was calculated at each time point and for each identified defect region using a grayscale-based automated segmentation process. The segmentation consisted

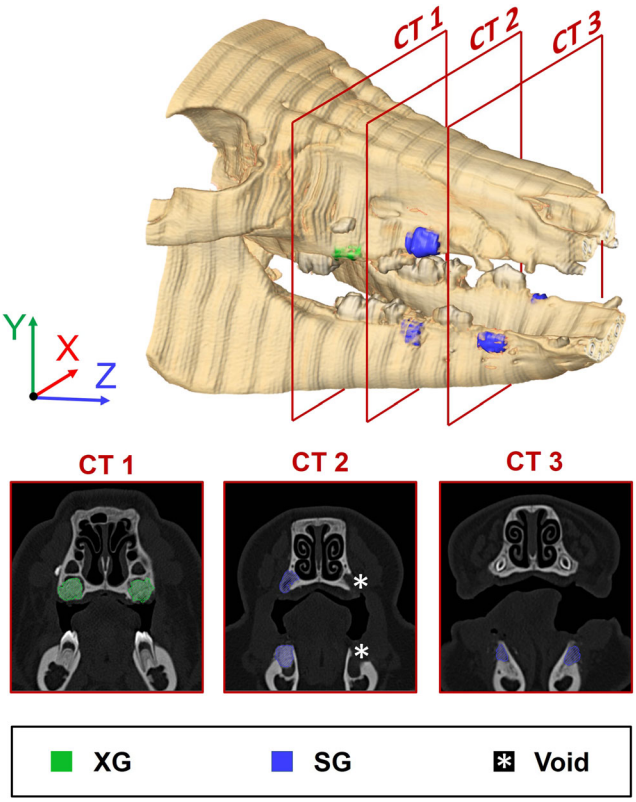

Fig. 2 Top: Reconstruction of the CT scan and grey values 3D segmentation of the different three-wall bone defects. Bottom: Three representative slices of the CT scan representing the segmentation of the different bone substitutes

in performing grey-value thresholding followed by an erosion-dilation filtering operation to remove segmentation artefacts external to the grafted region bulk and, finally, running an algorithm to fill the holes on the segmented region to eliminate possible pores inside the grafted region.

The grafted volumes of each defect at each time point were calculated with the following equation [23]:

$$V_k = \sum_{i=0}^{n} A_{k,i} \cdot \Delta z \ (k = 0, 6, 12\ ) \quad (1)$$

where V_k corresponds to the total grafted volume at each time point (i.e. $k = 0$, 6, or 12 weeks after surgery), $A_{k,i}$ is the grafted area calculated for one slice of the stack (i) at one time point (k), and Δz represents the elemental increment in the z scan direction (Fig. 2) determined by the CT configuration (i.e. 500 μm). The percent variation of the grafted volume (ΔV) after 6 or 12 weeks for the XG and SG was calculated using Eq. 2:

$$\Delta V = \frac{V_f - V_0}{V_0} \cdot 100\ [\%] \quad (2)$$

where V_0 corresponds to the volume of the grafted region in the initial CT scan (1 day after surgery, $k = 0$) and V_f

corresponds to the volume of the grafted region at the final time point (euthanised either at $k = 6$ or $k = 12$ weeks), calculated with Eq. 1. The segmentation and quantification process was performed with the image analysis software BoneJ (BoneJ, Fiji, ImageJ [24]) in a randomised blinded configuration.

Four samples (corresponding to the conditions 6w-XG-ULP, 6w-SG-LLP, 12w-SG-LRA, 12w-SG-LLA) were dismissed as the grafted region could not be clearly identified.

Histological analysis

After explantation, four randomly selected samples per BG group and regeneration time were chosen for micromorphological analysis. For this purpose, samples underwent the following process: First, the explanted samples were kept in a 4% formaldehyde solution for 1 week. Then, the defect regions were cut (diamond band saw, Exakt 300, EXAKT Technologies, Norderstedt, Germany) parallel to the coronal plane in 10 to 15 mm pieces. The samples were dehydrated by immersion in increasing ethanol concentrations of 30, 70, 80, 90, and 100% in water. Then, ethanol was gradually replaced by methyl methacrylate resin (Tecnovit 7200 VLC, Kulzer, Hanau, Germany) in successive solutions of 30, 70, 80, 90, and 100% in ethanol to ensure a complete infiltration. During all the resin infiltration process, samples were kept in a dark environment under vacuum. Samples were then polymerised (Photopolymerisation lamp, Exakt 520, EXAKT Technologies, Norderstedt, Germany), and the resulting blocks were cut in multiple 300 μm slices with the band saw and polished down to 30–50 μm (Micro grinder, Exakt 400 CS & Exakt AW110, EXAKT Technologies, Norderstedt, Germany). One slice per sample was stained using Masson–Goldner trichrome staining. Stained samples were observed using a bright-field optical microscope (AF7000, Leica, Switzerland) with and without a polarising filter. Another slice was coated with a thin carbon layer and observed in a scanning electron microscope (SEM, JEOL JSM-6510, Tokyo, Japan) with a backscattered electron detector (BSD).

Statistical analysis

The results of the volumetric CT quantification were processed through a statistical analysis software (Minitab 18.1, Minitab Inc., PA, USA) focusing on obtaining a global perspective of the role of each of the recorded surgery factor in the bone regeneration.

Firstly, all the data were checked for normal distributions and equivalence of variances (i.e. homoscedasticity) (Supplementary information: Least squares assumptions validation). Subsequently, an outlier test was run to remove possible outliers (Supplementary information: Outlier test). One outlier was found (for the condition 12 weeks, XG) and excluded from the statistical analysis. Then, a linear mixed-effects model (LMM) was fit to further understand the influence of the different factors on the grafted volume preservation (i.e. observed response). Such model allowed to consider both fixed and random effects [25]. The type of bone graft, regeneration time, jaw type (i.e. mandible vs maxilla), and anatomic site within each jaw (i.e. anterior or posterior) were included in the LMM as fixed effects, whereas the animal was included as a random effect (Table 1). Second- and third-order interactions between factors were also included in the model. The estimation method of this process followed the least-squares criterion. The correlations between factors were considered in the model. Most of the factors presented a cross-correlation due to the balanced design of the study and the random assignation of the defect anatomic sites to the different bone grafts. The exception was the unavoidable correlation between each animal and the corresponding regeneration time assigned. The nesting of these two factors was included in the LMM. During the fitting process, first, the third-order interactions with a p-value above the significance level (set to 5%) were excluded from the model. Then, the same procedure was repeated with the second-order interactions. Finally, the same was carried out with the main factors (Supplementary information: Linear mixed-effects model fitting).

Results

Computerised tomography

Qualitative CT evaluation

None of the grafts was lost during the healing period, and both BGs presented a stable filling of the granules inside the defects. It was also observed that the surgical procedure effectively reduced the buccal bone plate by half and preserved the lingual bone plate. The radiopacity of the SG was higher than that of the XG, as shown in Fig. 3. In addition, no bone regeneration was found in the empty defects, suggesting that they were critical-sized, and for this reason, they are not included in the following results.

Table 1 Factors included in the linear mixed-effects model and corresponding levels and reference names

	Factor	Levels	Ref.
Fixed factors	Bone graft (BG)	Synthetic graft/xenograft	SG/XG
	Regeneration time	6 weeks/12 weeks	6w/12w
	Jaw	Upper/lower	U/L
	Anatomic site	Anterior/posterior	A/P
Random factors	Animal	1–8	1–8

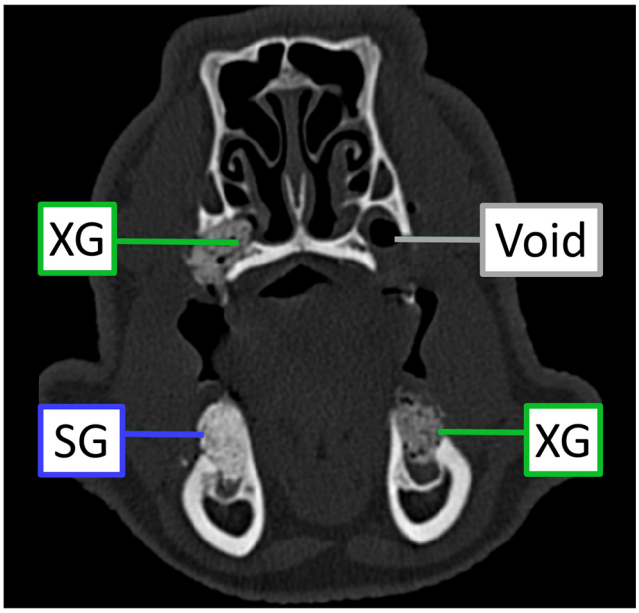

Fig. 3 Coronal slice of a CT scan showing four premolar grafted defects

Quantitative CT results

The data were analysed using a linear mixed-effects model, considering all the fixed effects (including their second- and third-order interactions) and the random effects. The non-statistically significant factors were successively removed until fitting a model with only significant factors. The parameters that were found to be significant were all the main factors, except "Jaw" type. The results of the fitted linear mixed-effects model are displayed in Table 2, and the main effects plot is shown in Fig. 4.

Additionally, the results of the variation of grafted bone volume are plotted as a function of the BG type and the regeneration time (Fig. 5). After 6 weeks, bone preservation percentages (mean value ± standard deviation) of − 30.81 ± 17.13% and − 10.82 ± 27.32% were observed for the XG and the SG, respectively. After 12 weeks, these percentages increased by approximately 16% being − 14.68 ± 29.17% and 5.72 ± 22.67% for the XG and the SG, respectively, which overall demonstrates better volume preservation by the SG.

Table 2 Linear mixed-effect model fit: *p*-value indicating the significance of each factor in the model. Determination of the positive-negative effect on the response for each level of each factor (+/− effect). Coefficient of each factor in the fitted regression equation. (The complete process can be found in the Supplementary information: Linear mixed-effects model fitting)

Factor	*p*-value	+ Effect	− Effect	Coef.
Bone Graft (BG)	0.001	SG	XG	11.83
Anatomic Site	0.028	A	P	7.61
Regeneration Time	0.037	12w	6w	7.20
Constant	0.002	N/A	N/A	− 10.84

Qualitative histological evaluation

The histological evaluation (Fig. 6) revealed the biocompatibility of the two bone grafts. No signs of inflammation, degeneration areas, nor bone necrosis was observed at any time point. Moreover, an active process of new bone formation was observed in both BGs, which showed osteoconductive properties and excellent osseointegration. This active new bone formation was observed with approximately the same intensity after 6 and 12 weeks in both biomaterials. After 6 weeks, most of the samples showed thin bone trabeculae with irregular alveolar bone crests and no corticalisation. At 12 weeks, a higher number of samples presented thick bone trabeculae and smooth alveolar crests.

Additionally, the histological slides were observed by linearly polarised light (LPL). LPL images allow identifying birefringent materials, which display optical anisotropy. In birefringent materials, the differences in light refraction result in variations of brightness, whereas materials without this feature are seen as opaque. Collagen is easily identified through LPL due to its birefringent properties [26]. In Fig. 6, several regions with varying brightness corresponding to the oriented collagen fibres were observed. Whilst in SGs one could notice this phenomenon occurring only in newly formed bone, in XGs the granules were also bright, which can be attributed to its biological origin.

A closer observation of the histological slides of the SG at 12 weeks revealed some resorption areas (indicated with black arrows in Fig. 7a, b in the outline of the vascular spaces between the biomaterial granules. The altered morphology of some of the granules contrasted with the original spheroidal morphology (presented in Fig. 7c) and was ascribed to osteoclastic resorption of the material.

The SEM images of the samples (Fig. 8) evidenced for both BGs an excellent osseointegration, with the newly formed bone not only surrounding the grafts but in direct contact with them. Additionally, lamellar bone was found around the Haversian canals (asterisks) in all samples. No differences in bone quantity and distribution were observed between 6 and 12 weeks nor between the BG type used (Fig. 8, Row a). Mature bone with Haversian structure was found in the grafted regions in all BGs. Osteons were clearly visible, with the Haversian canal surrounded by concentric bone lamellae and an interconnected network of osteocyte lacunae (white arrows) in the adjacent woven bone (Fig. 8, Row b).

Higher magnification images (Fig. 8, Row c) revealed the differences in microstructure of the two BGs. With a lamellar structure and the presence of some pores associated to osteocyte lacunae, the XG showed the typical microstructure of bone, due to its xenogenic origin. SGs, on the other hand,

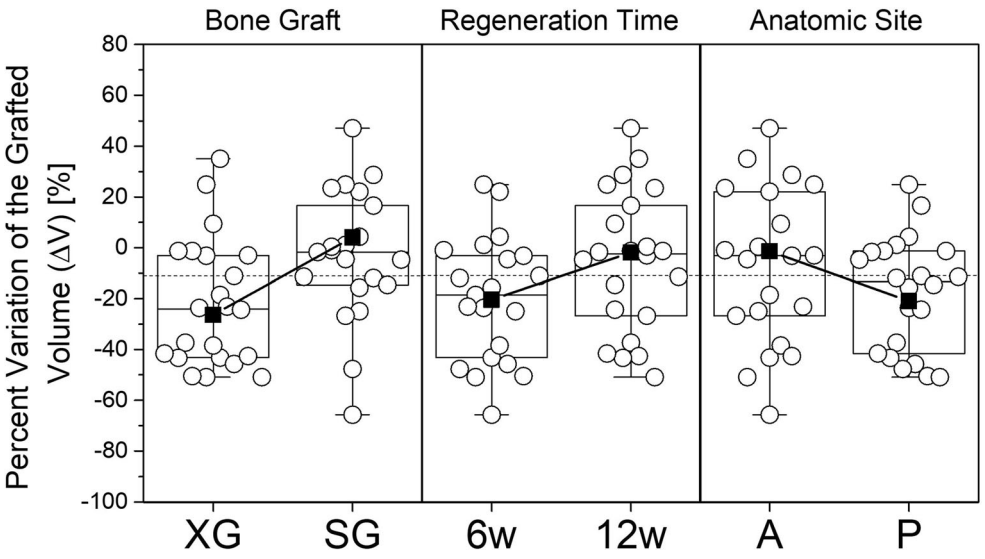

Fig. 4 Individual experimental observations (white dots) of the percent variation of the grafted volume (ΔV) grouped by the different significant factors according to the linear mixed-effects model (i.e. BG type, regeneration time, and anatomic site). Boxplot indicating the median and quartiles of the observed population distribution. Overlayed main effects plot (solid squares and trendlines) illustrating the mean responses for each level of the factors fitted in the model (Table 2). Constant coefficient represented in a horizontal dashed line

had a more porous microstructure, which resulted from the entangled network of calcium-deficient hydroxyapatite nanocrystals obtained during the biomimetic fabrication process [27, 28]. Moreover, it was observed that the new bone surrounding the XG fragments was woven bone, whereas more mature lamellar structures were seen in direct contact with the SG granules.

Discussion

Volume stability is critical, not only to avoid the implant neck or thread exposure but also to ensure treatment predictability and long-term success of the tooth reconstruction [29]. This study compares the performance, in terms of volume preservation, of two different bone grafts in a three-wall alveolar ridge defect in Landrace minipigs after 6 and 12 weeks. This type of bone defect has been widely studied in the literature [30, 31] and represents a more challenging situation compared to four-wall defects [32], but without reaching the complexity of vertical or horizontal bone augmentations.

The potential of biomimetic calcium phosphates for bone augmentation applications was assessed in a previous study, which evaluated the vertical bone formation of the same bone grafts tested in the present work, on the calvaria of rats [21]. Faster bone regeneration was observed for the biomimetic SG group compared to XGs. However, the relevance of that indication for clinical research is limited [33]. Therefore, in the

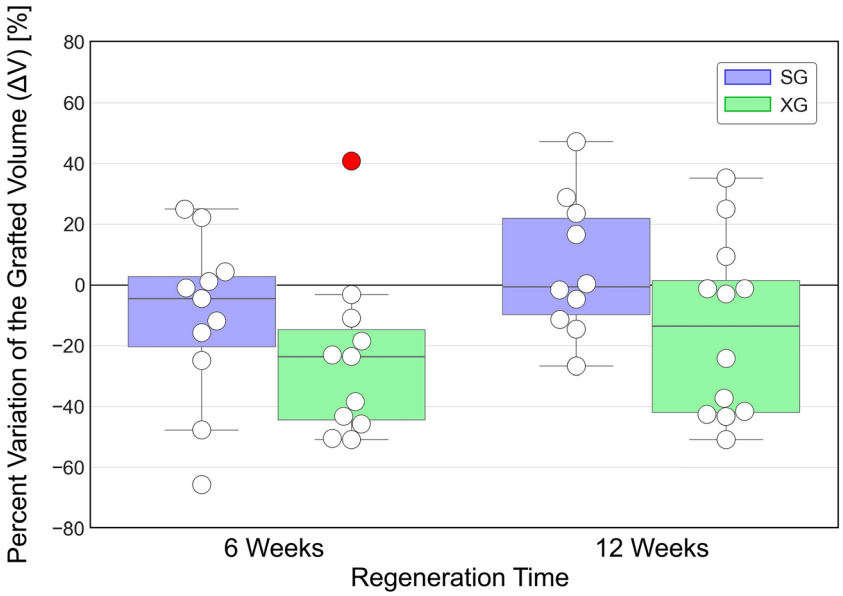

Fig. 5 Percent variation of the grafted volume (ΔV) for the different BG types (SG and XG) after 6 and 12 weeks of regeneration. Boxplots superimposed to scatterplots with white points representing the analysed data and red points representing the outliers.

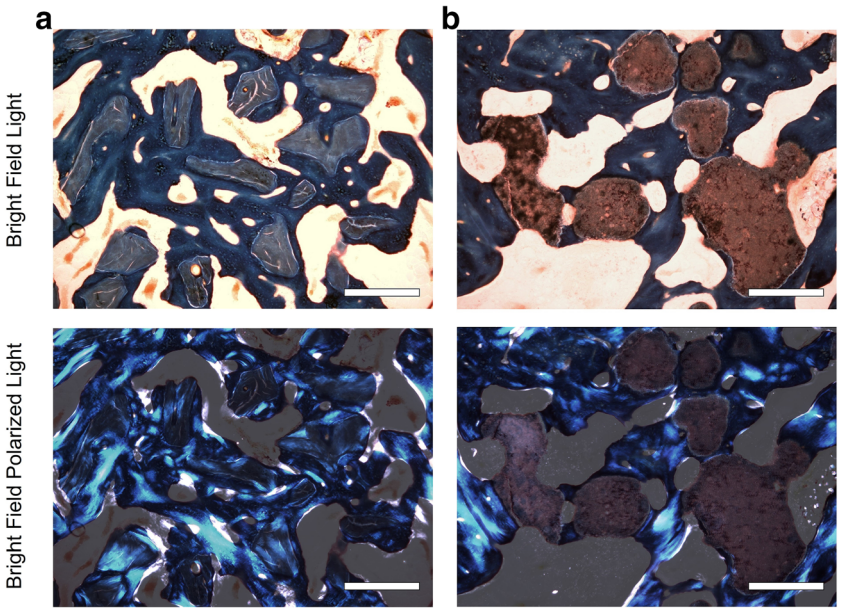

Fig. 6 Histological views showing the grafted regions with XG (**a**) and SG (**b**) after 12 weeks of regeneration stained with Masson–Goldner trichrome technique. Top: Bright field light microscopy where the newly formed bone appears in blue, the XG in grey, and the SG in brown. Bottom: Bright field polarised light microscopy images (with overlaid original image at 75% of transparency) of the same region evidencing the collagen orientation in the forming bone. Scale bars represent 500 μm

present study, the material was tested in a large animal model, in an indication that is more similar to the clinical situation. In fact, minipigs are considered to be an animal model much closer to humans, not only in terms of the anatomy and composition of bone tissue but also in terms of the bone regeneration and remodelling process [34].

The primary outcome of the study, 3D-volume preservation by CT analysis, was defined to match the current follow-up technique of bone grafting procedures in the dental offices, with the goal of resembling the clinical setup. It is common in preclinical and clinical studies in the dental field to use radiological data as the main outcome [12, 13, 35, 36].

A linear mixed-effects model data analysis allowed identifying the effect of each parameter on the preservation of the grafted bone volume as well as the existence of possible interactions between them. Randomisation and a high number of replicates allowed this approach. Interestingly, the type of bone graft used resulted to be the most influential parameter, followed by the anatomic site and the regeneration time, which had a similar influence. By contrast, the placement of the defect in either the mandible or the maxilla was not found to have a significant effect. The levels of each factor in the mixed-effects model that resulted in higher bone preservation were synthetic grafts, longer regeneration times (i.e. 12 weeks), and anterior positions. Regarding the effect of bone graft in the volume preservation, the SG presented a limited volume loss of around 11% on average at 6 weeks and a volume gain of 6% at 12 weeks, whereas the xenograft lost between 31 and 15% of the initial grafted volume at 6 and 12 weeks, respectively (Fig. 5). These findings regarding the XG are in agreement with previous studies [12, 13, 37, 38] and may be attributed to the packing of the xenograft flakes, as schematised in Fig. 9, rather than to a resorption process, which is known to be very limited for this bone substitute

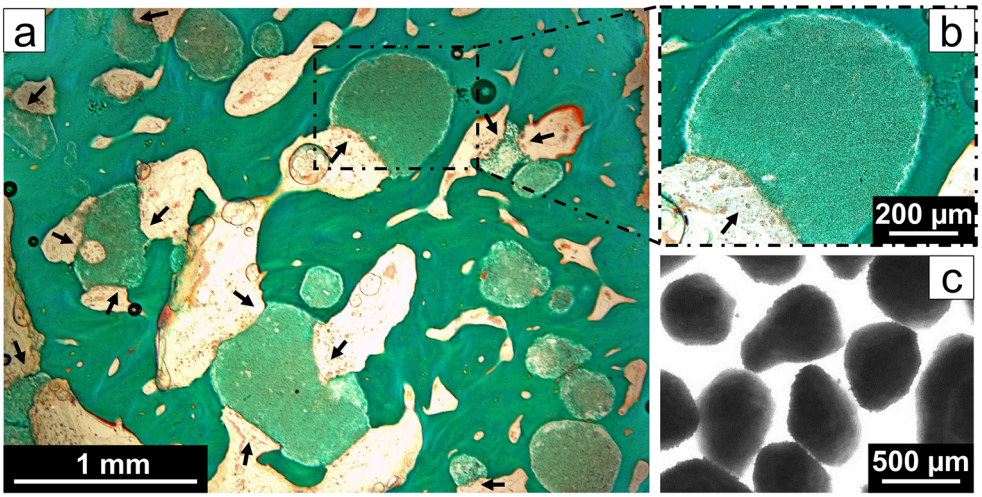

Fig. 7 **a, b** Histological section stained with Masson's trichrome showing a defect grafted with SG at 12 weeks post-surgery. Arrows indicate the regions where the rounded morphology of the BG has been altered by the osteoclastic resorption. **c** Optical microscopy image showing the morphology of the SG granules before surgery

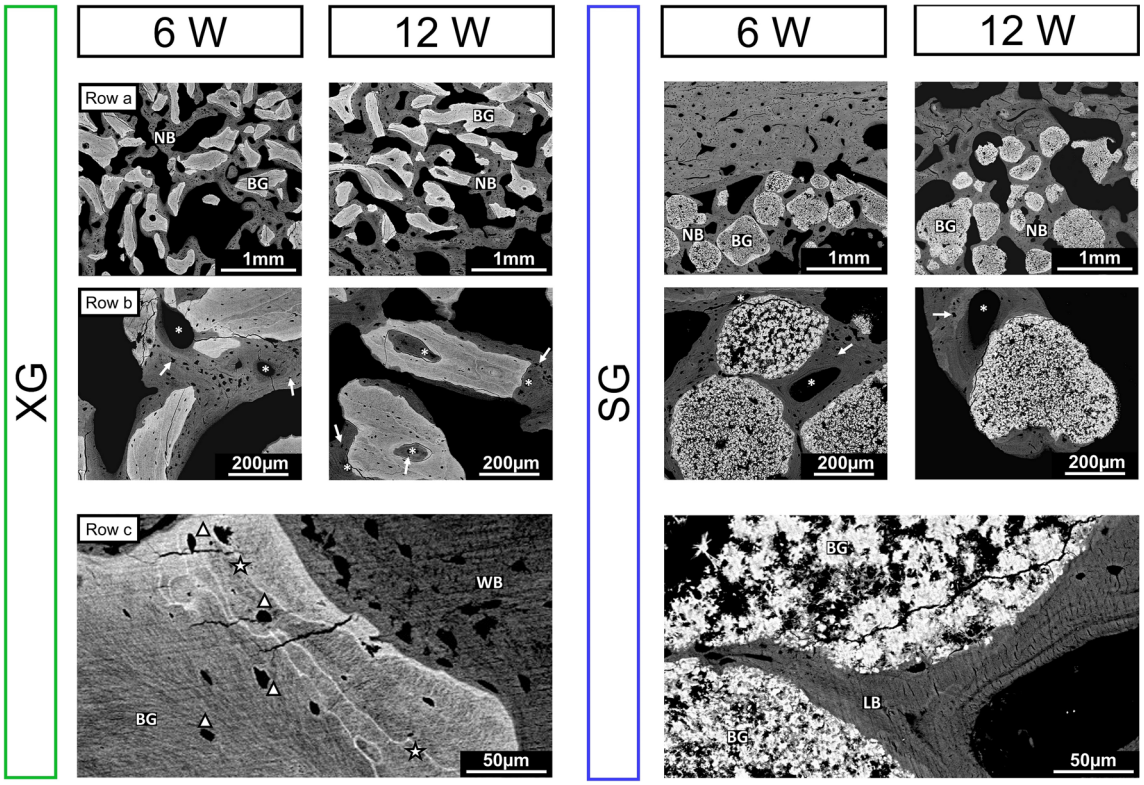

Fig. 8 SEM images of grafted regions after 6 and 12 weeks of surgery. Row **a**: Lower magnification micrographs showing the good integration between the bone graft (BG) and newly formed bone (NB). Row **b**: Higher magnification images allow identifying the Haversian canals (asterisks) and osteocyte lacunae (arrows) indicating the presence of osteons and of a mature bone structure in both BGs. Row **c**: A closer look into the BGs reveals the different microstructures. On the XG one can observe osteocyte lacunae (triangles) and mineralisation bands (star) of the original bovine bone constituting the biomaterial, in a lighter shade than the newly formed woven bone (WB) surrounding it. In the SG, it is possible to distinguish the calcium-deficient hydroxyapatite (CDHA) nano-crystal network typical of biomimetic calcium phosphates, surrounded by a new bone deposit with a lamellar structure (LB)

[39]. This packing process may only occur soon after surgery, when the biomaterial is not osseointegrated, and explains why Younes et al. observed a reduction in the grafted volume only during the first 3 months, remaining stable thereafter (up to 2 years) [38]. Moreover, the fact that the regeneration time was also statistically significant and had a positive influence on the regenerated bone volume can be attributed to the natural bone remodelling process occurring in the bone defects. Finally, the mixed-effects model revealed also a significant effect of the anatomic site, with better volume preservation on anterior positions. Although it is not clear that the results can be extrapolated across species, this finding is in agreement with previous studies in dental research reporting a higher turnover rate in anterior alveolar bone, associated to the higher ratio of trabecular bone [40].

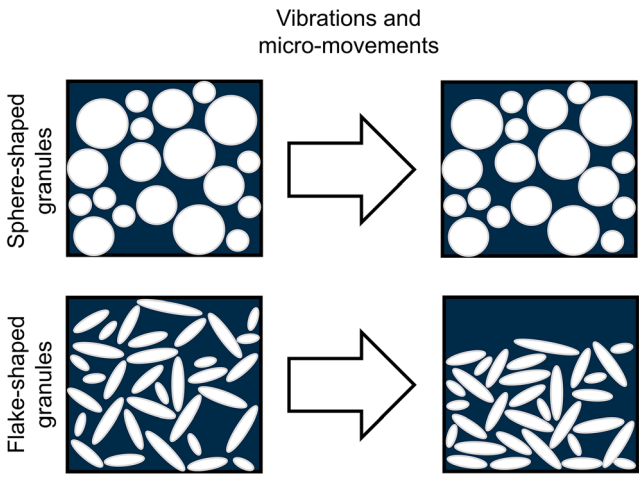

Fig. 9 Schema representing the packing effect of different granules morphologies after vibrations and micromovements

The histological observations proved that both biomaterials had excellent osteointegrative properties and biocompatibility, since a direct bone ingrowth on the particles was observed without any graft encapsulation. The Haversian bone structure observed in the samples indicated a mature stage of bone remodelling with stress-oriented tissue, thus denoting a mechanically stable architecture [41]. The presence of these structures through the whole sample at the shortest time point (6 weeks) supported the high osteoconductivity on both BG types. Additionally, the biomimetic synthetic grafts presented newly formed bone in a more mature stage than the

xenografts in the regions surrounding the biomaterial, suggesting a faster remodelling process.

As far as degradation is concerned, biomimetic synthetic bone grafts with very similar compositions and microstructures to the SG analysed in the current study have been shown to sustain cell-mediated degradation [42, 43], as demonstrated by the observation of the typical Howship's lacunae and cutting cones in close contact with the materials. In the same vein, Mai et al. observed, in a miniature swine mandible model grafted with an apatitic bone cement, that the biomaterial underwent a process of resorption that occurred simultaneously to bone formation [44]. This is consistent with the observation of concave morphologies in the SGs in the present study (Fig. 7), compatible with osteoclastic resorption. However, this did not lead to a volume shrinkage at 12 weeks, but rather the opposite, which suggests that the SG resorption was incorporated in the physiological remodelling process of natural bone. This hypothesis is further supported by the mature lamellar structures found in direct contact with the SG (Fig. 8, Row c), in contrast to the woven bone surrounding the XG (Fig. 8, Row c).

Regarding the biodegradation of the XG, this is in fact a controversial topic in the literature. Numerous clinical studies report proper osseointegration and bone regeneration but a slow or inexistent degradability. Skoglund et al. performed alveolar ridge augmentation procedures and observed non-resorbed particles after 44 months, showing doubts as to whether the material should be considered resorbable [45]. Similar observations were done by Duda et al. after a 30-month study [46]. In a longer-term study, Schlegel et al. described the absence of clinical or histological signs of granule resorption after 6 years [47], nor was the degradation of the XG observed in other studies combining the XG with autologous bone (80/20 mixture). For instance, Hallman et al. did not find signs of resorption after 6 months in maxillary sinus floor augmentation [48], and Mordenfeld et al. concluded, through histomorphometric measurements, that no significant changes in the particle size were observed after 11 years in maxillary sinus augmentation procedures [39]. However, other studies have reported cell-mediated degradation for this same material [49–52]. The discrepancies in the results could be attributed to different factors, such as the grafting site or the local mechanical environment. In this respect, Araújo et al. tested an orthodontic procedure to move a tooth into a XG-grafted region in a canine model, concluding that there was a tension-dependent resorption of the material. Whilst in the unloaded regions the graft remained unaltered, in the regions adjacent to the tooth subjected to mechanical stress the osteoclastic resorption of the granules was accentuated [53]. In the present study, the histological assessment provided no evidence of XG resorption. This contrasts with a previous work that used the same animal model and defect location, where cell-mediated resorption was identified in the histological studies of the same XG [54]. An important point to consider is that the size of the defect was considerably larger ($30 \times 15 \times 13$ mm^3) than the one used in the present study. As the defect size undoubtedly influences the biomechanical stimuli that the graft receives, this could be the cause of the discrepancies between the two studies.

Determining more in depth the role of each bone graft in the bone regeneration process would require additional characterisation techniques [55], which are beyond the scope of this study. For instance, performing immunohistochemical staining of some selected decalcified samples would allow to better assess the osteoclastic activity around the BG granules and better understand the resorption process in both conditions. Additionally, by real-time polymerase chain reaction (qPCR) the gene expression of key genes for bone regeneration (e.g. type I collagen, ALP, osteonectin, osteocalcin, BMP-2, and osteopontin) could be quantitatively assessed and compared between the two BGs.

One last aspect to consider, regarding the scope and limitations of this study, is that we opted to perform standardised defects in order to guarantee a more comparable scenario and reduce as much as possible the variability associated with defect morphology. However, this is achieved at the expense of renouncing to use a chronified model, which would be more representative of the common clinical situation. Moreover, it would be interesting to address the mechanical stability of the grafted region and the interaction with dental implants, which are important aspects of the bone graft performance that should be considered in future studies.

In summary, the efficacy of two commercially available bone grafts was assessed in a preclinical study, mimicking the clinical setup of a three-wall defect in the alveolar crest. The two BGs analysed showed excellent osteoconduction, guiding the formation of new bone in the defect. Additionally, the results obtained from the three-dimensional CT scan analysis revealed that volume preservation was better achieved with the biomimetic synthetic graft, suggesting that the morphology of the granules plays an important role in this respect.

Supplementary Information The online version contains supplementary material available at https://doi.org/10.1007/s00784-021-03956-y.

Acknowledgements Y.R. acknowledges the Spanish Government for the PhD grant DI-15-08184 and M.-P.G. the Generalitat de Catalunya for the ICREA Academia Award. The authors kindly acknowledge the collaboration of the Serveis Científico-Tècnics SEM Team of the University of Barcelona. The authors thank Christian Guirola for proofreading the text.

Author contribution D.P. and Y.M. designed the study; I.G. performed the surgeries; Y.R. and M.O. processed the samples; Y.R., D.P., Y.M., M.O., and M-C.M. collected the data; Y.R., D.P., and M.-P.G. analysed the results and wrote the manuscript.

Funding This study was supported by Mimetis Biometerials S.L., Barcelona, Spain.

Declarations

Ethical approval Ethical approval was obtained from the Specipig Ethics Committee for Animal Experimentation (Specipig S.L., Barcelona, Spain).

ARRIVE guidelines This study has been carried out in compliance with the ARRIVE guidelines for the reporting of in-vivo experiments in animal research. The ARRIVE checklist can be found in the supplementary information.

Conflict of interest Y.R., D.P., Y.M., and M.-P. G. have an equity interest in Mimetis Biomaterials, S.L., a spin-off company of UPC that may potentially benefit from the research results displayed in the present work.

References

1. Duncan RL, Turner CH (1995) Mechanotransduction and the functional response of bone to mechanical strain. Calcif Tissue Int 57: 344–358. https://doi.org/10.1007/BF00302070
2. Araujo MG, Lindhe J (2005) Dimensional ridge alterations following tooth extraction. An experimental study in the dog. J Clin Periodontol 32:212–218. https://doi.org/10.1111/j.1600-051X.2005.00642.x
3. Esposito M, Grusovin MG, Coulthard P, Worthington HV The efficacy of various bone augmentation procedures for dental implants: a Cochrane systematic review of randomized controlled clinical trials. Int J Oral Maxillofac Implants 21:696–710
4. Greenwald AS, Boden SD, Goldberg VM, Khan Y, Laurencin CT, Rosier RN, American Academy of Orthopaedic Surgeons. The Committee on Biological Implants (2001) Bone-graft substitutes: facts, fictions, and applications. J Bone Jt Surg-Am Vol 83:98–103. https://doi.org/10.2106/00004623-200100022-00007
5. Zeugolis DI, Keeney M, Collin E, et al (2011) Xenogenic tissues and biomaterials for the skeletal system. In: Comprehensive Biomaterials. Elsevier, pp 387–404
6. Kunert-Keil C, Gredes T, Gedrange T (2011) Biomaterials applicable for alveolar sockets preservation: in vivo and in vitro studies. In: Implant Dentistry - The Most Promising Discipline of Dentistry. InTech
7. Precheur HV (2007) Bone graft materials. Dent Clin N Am 51:729–746. https://doi.org/10.1016/j.cden.2007.03.004
8. Ginebra M-P, Espanol M, Maazouz Y et al (2018) Bioceramics and bone healing. EFORT Open Rev 3:173–183. https://doi.org/10.1302/2058-5241.3.170056
9. Sadowska JM, Wei F, Guo J, Guillem-Marti J, Ginebra MP, Xiao Y (2018) Effect of nano-structural properties of biomimetic hydroxyapatite on osteoimmunomodulation. Biomaterials 181:318–332. https://doi.org/10.1016/j.biomaterials.2018.07.058
10. Barba A, Maazouz Y, Diez-Escudero A, Rappe K, Espanol M, Montufar EB, Öhman-Mägi C, Persson C, Fontecha P, Manzanares MC, Franch J, Ginebra MP (2018) Osteogenesis by foamed and 3D-printed nanostructured calcium phosphate scaffolds: effect of pore architecture. Acta Biomater 79:135–147. https://doi.org/10.1016/j.actbio.2018.09.003
11. Barba A, Diez-Escudero A, Maazouz Y, Rappe K, Espanol M, Montufar EB, Bonany M, Sadowska JM, Guillem-Marti J, Öhman-Mägi C, Persson C, Manzanares MC, Franch J, Ginebra MP (2017) Osteoinduction by foamed and 3D-printed calcium phosphate scaffolds: effect of nanostructure and pore architecture. ACS Appl Mater Interfaces 9:41722–41736. https://doi.org/10.1021/acsami.7b14175
12. Kirmeier R, Payer M, Wehrschuetz M, Jakse N, Platzer S, Lorenzoni M (2008) Evaluation of three-dimensional changes after sinus floor augmentation with different grafting materials. Clin Oral Implants Res 19:366–372. https://doi.org/10.1111/j.1600-0501.2007.01487.x
13. Mazzocco F, Lops D, Gobbato L et al (2014) Three-dimensional volume change of grafted bone in the maxillary sinus. Int J Oral Maxillofac Implants 29:178–184. https://doi.org/10.11607/jomi.3236
14. Schilling AF, Linhart W, Filke S, Gebauer M, Schinke T, Rueger JM, Amling M (2004) Resorbability of bone substitute biomaterials by human osteoclasts. Biomaterials 25:3963–3972. https://doi.org/10.1016/j.biomaterials.2003.10.079
15. Sadowska JM, Ginebra M-P (2020) Inflammation and biomaterials: role of the immune response in bone regeneration by inorganic scaffolds. J Mater Chem B 8:9404–9427. https://doi.org/10.1039/D0TB01379J
16. Thomas MV, Puleo DA (2011) Infection, inflammation, and bone regeneration: a paradoxical relationship. J Dent Res 90:1052–1061. https://doi.org/10.1177/0022034510393967
17. Hankenson KD, Dishowitz M, Gray C, Schenker M (2011) Angiogenesis in bone regeneration. Injury 42:556–561. https://doi.org/10.1016/j.injury.2011.03.035
18. Flautre B, Descamps M, Delecourt C, Blary MC, Hardouin P (2001) Porous HA ceramic for bone replacement: role of the pores and interconnections—experimental study in the rabbit. J Mater Sci Mater Med 12:679–682. https://doi.org/10.1023/A:1011256107282
19. Rustom LE, Boudou T, Nemke BW, Lu Y, Hoelzle DJ, Markel MD, Picart C, Wagoner Johnson AJ (2017) Multiscale porosity directs bone regeneration in biphasic calcium phosphate scaffolds. ACS Biomater Sci Eng 3:2768–2778. https://doi.org/10.1021/acsbiomaterials.6b00632
20. Hench LL, Wilson J (1993) An introduction to bioceramics. World Scientific Pub Co Inc
21. Hoornaert A, Maazouz Y, Pastorino D, Aparicio C, de Pinieux G, Fellah BH, Ginebra MP, Layrolle P (2019) Vertical bone regeneration with synthetic biomimetic calcium phosphate onto the calvaria of rats. Tissue Eng Part C Methods 25:1–11. https://doi.org/10.1089/ten.tec.2018.0260
22. Rissolo AR, Bennett J (1998) Bone grafting and its essential role in implant dentistry. Dent Clin N Am 42:91–116
23. Uchida Y, Goto M, Katsuki T, Soejima Y (1998) Measurement of maxillary sinus volume using computerized tomographic images. Int J Oral Maxillofac Implants 13:811–818
24. Doube M, Klosowski MM, Arganda-Carreras I et al (2010) BoneJ: Free and extensible bone image analysis in ImageJ. Bone 47:1076–1079. https://doi.org/10.1016/j.bone.2010.08.023
25. Pinheiro JC, Bates DM (2000) Mixed-effects models in S and S-PLUS. Springer-Verlag, New York
26. Bromage TG, Goldman HM, McFarlin SC et al (2003) Circularly polarized light standards for investigations of collagen fiber orientation in bone. Anat Rec 274B:157–168. https://doi.org/10.1002/ar.b.10031
27. Ginebra MP, Fernández E, De Maeyer EAP et al (1997) Setting reaction and hardening of an apatitic calcium phosphate cement. J Dent Res 76:905–912. https://doi.org/10.1177/00220345970760041201
28. Roveri N, Iafisco M (2010) Evolving application of biomimetic nanostructured hydroxyapatite. Nanotechnol Sci Appl 107. https://doi.org/10.2147/NSA.S9038

29. Jemt T, Lekholm U (2003) Measurements of Buccal tissue volumes at single-implant restorations after local bone grafting in maxillas: a 3-year clinical prospective study case series. Clin Implant Dent Relat Res 5:63–70. https://doi.org/10.1111/j.1708-8208.2003.tb00185.x
30. Oltramari PVP, de Lima NR, Henriques JFC et al (2007) Evaluation of bone height and bone density after tooth extraction: an experimental study in minipigs. Oral Surg Oral Med Oral Pathol Oral Radiol Endod 104:e9–e16. https://doi.org/10.1016/j.tripleo.2007.06.015
31. Ruehe B, Niehues S, Heberer S, Nelson K (2009) Miniature pigs as an animal model for implant research: bone regeneration in critical-size defects. Oral Surg Oral Med Oral Pathol Oral Radiol Endod 108:699–706. https://doi.org/10.1016/j.tripleo.2009.06.037
32. Misch CE, Suzuki JB (2008) Tooth extraction, socket grafting, and barrier membrane bone regeneration. In: Contemporary Implant Dentistry, 3rd ed. pp 870–904
33. Li Y, Chen S-K, Li L, Qin L, Wang XL, Lai YX (2015) Bone defect animal models for testing efficacy of bone substitute biomaterials. J Orthop Transl 3:95–104. https://doi.org/10.1016/j.jot.2015.05.002
34. Wang S, Liu Y, Fang D, Shi S (2007) The miniature pig: a useful large animal model for dental and orofacial research. Oral Dis 13:530–537. https://doi.org/10.1111/j.1601-0825.2006.01337.x
35. Dasmah A, Thor A, Ekestubbe A, Sennerby L, Rasmusson L (2012) Particulate vs. block bone grafts: three-dimensional changes in graft volume after reconstruction of the atrophic maxilla, a 2-year radiographic follow-up. J Cranio-Maxillofac Surg 40:654–659. https://doi.org/10.1016/j.jcms.2011.10.032
36. Jensen T, Schou S, Svendsen PA, Forman JL, Gundersen HJG, Terheyden H, Holmstrup P (2012) Volumetric changes of the graft after maxillary sinus floor augmentation with Bio-Oss and autogenous bone in different ratios: a radiographic study in minipigs. Clin Oral Implants Res 23:902–910. https://doi.org/10.1111/j.1600-0501.2011.02245.x
37. Salem D, Alshihri A, Arguello E et al (2019) Volumetric analysis of allogeneic and xenogeneic bone substitutes used in maxillary sinus augmentations utilizing cone beam computed tomography: a prospective randomized pilot study. Int J Oral Maxillofac Implants 34:920–926. https://doi.org/10.11607/jomi.7318
38. Younes F, Cosyn J, De Bruyckere T et al (2019) A 2-year prospective case series on volumetric changes, PROMs, and clinical outcomes following sinus floor elevation using deproteinized bovine bone mineral as filling material. Clin Implant Dent Relat Res 21:301–309. https://doi.org/10.1111/cid.12730
39. Mordenfeld A, Hallman M, Johansson CB, Albrektsson T (2010) Histological and histomorphometrical analyses of biopsies harvested 11 years after maxillary sinus floor augmentation with deproteinized bovine and autogenous bone. Clin Oral Implants Res 961–970. https://doi.org/10.1111/j.1600-0501.2010.01939.x
40. Sakka S, Coulthard P (2009) Bone Quality: A reality for the process of osseointegration. Implant Dent 18:480–485. https://doi.org/10.1097/ID.0b013e3181bb840d
41. Rho J-Y, Kuhn-Spearing L, Zioupos P (1998) Mechanical properties and the hierarchical structure of bone. Med Eng Phys 20:92–102. https://doi.org/10.1016/S1350-4533(98)00007-1
42. Barba A, Diez-Escudero A, Espanol M, Bonany M, Sadowska JM, Guillem-Marti J, Öhman-Mägi C, Persson C, Manzanares MC, Franch J, Ginebra MP (2019) Impact of biomimicry in the design of osteoinductive bone substitutes: nanoscale matters. ACS Appl Mater Interfaces 11:8818–8830. https://doi.org/10.1021/acsami.8b20749
43. Cuzmar E, Perez RA, Manzanares M-C, Ginebra MP, Franch J (2015) In vivo osteogenic potential of biomimetic hydroxyapatite/collagen microspheres: comparison with injectable cement pastes. PLoS One 10:e0131188. https://doi.org/10.1371/journal.pone.0131188
44. Mai R, Reinstorf A, Pilling E, Hlawitschka M, Jung R, Gelinsky M, Schneider M, Loukota R, Pompe W, Eckelt U, Stadlinger B (2008) Histologic study of incorporation and resorption of a bone cement–collagen composite: an in vivo study in the minipig. Oral Surg Oral Med Oral Pathol Oral Radiol Endod 105:e9–e14. https://doi.org/10.1016/j.tripleo.2007.09.016
45. Skoglund A, Hising P, Young C (1997) A clinical and histologic examination in humans of the osseous response to implanted natural bone mineral. Int J Oral Maxillofac Implants 12:194–199
46. Duda M, Pajak J (2004) The issue of bioresorption of the Bio-Oss xenogeneic bone substitute in bone defects. Ann Univ Mariae Curie Sklodowska Med 59(1):269–277
47. Schlegel A, Donath K (1998) BIO-OSS®—a resorbable bone substitute? J Long-Term Eff Med Implants 8(3–4):201–209
48. Hallman M, Cederlund A, Lindskog S, Lundgren S, Sennerby L (2001) A clinical histologic study of bovine hydroxyapatite in combination with autogenous bone and fibrin glue for maxillary sinus floor augmentation: results after 6 to 8 months of healing. Clin Oral Implants Res 12:135–143. https://doi.org/10.1034/j.1600-0501.2001.012002135.x
49. Tadjoedin ES, De Lange GL, Bronckers ALJJ et al (2003) Deproteinized cancellous bovine bone (Bio-Oss®) as bone substitute for sinus floor elevation. A retrospective, histomorphometrical study of five cases. J Clin Periodontol 30:261–270. https://doi.org/10.1034/j.1600-051X.2003.01099.x
50. Zaffe D, Leghissa GC, Pradelli J, Botticelli AR (2005) Histological study on sinus lift grafting by Fisiograft and Bio-Oss. J Mater Sci Mater Med 16:789–793. https://doi.org/10.1007/s10856-005-3574-5
51. McAllister BS, Margolin MD, Cogan AG, Buck D, Hollinger JO, Lynch SE (1999) Eighteen-month radiographic and histologic evaluation of sinus grafting with anorganic bovine bone in the chimpanzee. Int J Oral Maxillofac Implants 14:361–368
52. Sartori S, Silvestri M, Forni F, Icaro Cornaglia A, Tesei P, Cattaneo V (2003) Ten-year follow-up in a maxillary sinus augmentation using anorganic bovine bone (Bio-Oss). A case report with histomorphometric evaluation. Clin Oral Implants Res 14:369–372. https://doi.org/10.1034/j.1600-0501.2003.140316.x
53. Araújo MG, Carmagnola D, Berglundh T et al (2001) Orthodontic movement in bone defects augmented with Bio-Oss®. An experimental study in dogs. J Clin Periodontol 28:73–80. https://doi.org/10.1034/j.1600-051x.2001.280111.x
54. Rumpel E, Wolf E, Kauschke E, Bienengräber V, Bayerlein T, Gedrange T, Proff P (2006) The biodegradation of hydroxyapatite bone graft substitutes in vivo. Folia Morphol (Warsz) 65:43–48
55. Stein GS, Lian JB (1993) Molecular mechanisms mediating proliferation/differentiation interrelationships during progressive development of the osteoblast phenotype. Endocr Rev 14:424–442. https://doi.org/10.1210/edrv-14-4-424